ELSEVIER

Chemical Engineering Journal 91 (2003) 151–158

Chemical Engineering Journal

www.elsevier.com/locate/cej

Relaxation oscillations in a kinetic model of catalytic hydrogen oxidation involving a chase on canards

G.A. Chumakov [a,1], N.A. Chumakova [b,*]

[a] *Sobolev Institute of Mathematics, SB RAS, 630090 Novosibirsk, Russia*
[b] *Boreskov Institute of Catalysis, SB RAS, 630090 Novosibirsk, Russia*

Abstract

A detailed study of two- and three-variable mathematical models of a heterogeneous catalytic system is presented with special attention to weakly stable dynamics, a type of complex irregular behavior frequently encountered in oscillating chemical reactions. One of the most important properties of the weakly stable dynamics is "a sensitive dependence on the initial conditions". Our analysis of a global error in long-term numerical integration shows that a high sensitive dependence on the initial conditions appears in the three-variable system with fast, intermediate and slow variables due to existence of the canard cycles which occur close to Hopf bifurcation in the one-parameter family of two-variable subsystems.

Keywords: Hopf bifurcation; Kinetic model; Weak stability dynamics; Relaxation oscillations; Canards

1. Introduction

Relaxation oscillations characterized by two quite different time scales have been observed in physical, chemical and biochemical systems [1–3]. Investigation of relaxation and chaotic oscillations in many heterogeneous catalytic systems has been developed very rapidly during recent years [3–6]. Our renewed interest in relaxation oscillations [7] arose from the introduction and use of Non-Standard Analysis in the study of singular perturbations in applied problems. A major claim to fame for Non-Standard Analysis is the discovery of a new phenomenon in relaxation oscillations that was called "Les Canards" or "Ducks" by a group of French mathematicians [8,9].

In this paper, the Ducks will be chased in an one-parameter family of two-variable mathematical models of oscillating heterogeneous catalytic system, that is, our purpose here is to analyze numerically the transition from the harmonic oscillations near the Hopf bifurcation to large amplitude relaxation oscillations as the bifurcation parameter is varied. In effect, the range of the parameter is extremely small where the canard configurations are observed. We note that the canard configurations appearance is comparable with the simplest global (co-dimension one) bifurcations of periodic solutions of singularly perturbed systems. In other words, in the generic one-parameter family of two-variable dynamical systems it is an inherent peculiarity [10]. Hence, the canard appearance is not destroyed by the addition of a small smooth perturbation to the one-parameter family.

At the end of the paper, we will discuss the phenomenon of "weakly stable dynamics" [11] of the global reaction rate in the three-variable model with fast, intermediate and slow variables. Its connection with both the canard cycles in the one-parameter family of two-variable systems with fast and intermediate variables and the influence of the global error in long-term numerical integration of ordinary differential equations [12] as a source of stochastic effects will also be demonstrated.

Let us consider the mechanism of the heterogeneous reaction of hydrogen oxidation on metallic catalysts [13,14]:

$$\begin{aligned} &H_2 + 2[Me] \leftrightarrow 2[HMe] \\ &O_2 + 2[Me] \leftrightarrow 2[OMe] \\ &2[HMe] + [OMe] \rightarrow 3[Me] + H_2O \\ &H_2 + [OMe] \rightarrow [Me] + H_2O \\ &[Me_v] + [HMe] \leftrightarrow [Me_vH] + [Me] \\ &[Me_v] + [OMe] \leftrightarrow [Me_vO] + [Me] \end{aligned} \quad (1)$$

Here [Me] and $[Me_v]$ are a vacant active site on the catalyst surface and an atom in the subsurface layer, respectively, [HMe], [OMe] and $[Me_vH]$, $[Me_vO]$ are hydrogen and oxygen atoms adsorbed on the surface and dissolved into the

* Corresponding author. Tel.: +7-383-2-341-278.
E-mail addresses: chumakov@math.nsc.ru (G.A. Chumakov), chum@catalysis.nsk.su (N.A. Chumakova).
[1] Tel.: +7-383-2-334-129.

1385-8947/02/$ – see front matter
PII: S1385-8947(02)00148-1

subsurface layer of the catalyst. The last two steps in Scheme 1 are assumed to be slow in comparison to adsorption and reaction steps. We shall study the case when the activation energies of the third and fourth reaction steps may depend linearly upon the concentrations of the reactants in the subsurface layer and upon the concentration of oxygen adsorbed [3,4,13].

2. Mathematical model

The dynamic behavior of the catalytic system (1) is described by a set of six non-linear ordinary differential equations:

$$\begin{aligned}
\dot{x}_1 &= 2[k_1x_5(1-x_1-x_2)^2 - k_{-1}x_1^2 - k_3(\boldsymbol{x})x_1^2x_2] \\
&\quad -\beta_1\dot{x}_3, \\
\dot{x}_2 &= 2[k_2x_6(1-x_1-x_2)^2 - k_{-2}x_2^2] - k_3(\boldsymbol{x})x_1^2x_2 \\
&\quad -k_4(\boldsymbol{x})x_5x_2 - \beta_2\dot{x}_4, \\
\dot{x}_3 &= k_5x_1(1-x_3) - k_{-5}x_3(1-x_1-x_2), \\
\dot{x}_4 &= k_6x_2(1-x_4) - k_{-6}x_4(1-x_1-x_2), \\
\delta\dot{x}_5 &= -\delta\beta[k_1x_5(1-x_1-x_2)^2 - k_{-1}x_1^2 - k_4(\boldsymbol{x})x_5x_2] \\
&\quad +x_{50} - x_5, \\
\delta\dot{x}_6 &= -\delta\beta[k_2x_6(1-x_1-x_2)^2 - k_{-2}x_2^2] + x_{60} - x_6,
\end{aligned} \tag{2}$$

where x_1, x_2 are surface coverages by hydrogen and oxygen adsorbed on the metal surface, so that $x_1 \geq 0$, $x_2 \geq 0$, $x_1 + x_2 \leq 1$; x_3, x_4 the concentrations of hydrogen and oxygen dissolved into subsurface layer counted up as ratios to the upper limit-values of these concentrations, respectively, so that $0 \leq x_3 \leq 1$ and $0 \leq x_4 \leq 1$; x_5, x_6 are partial pressures of hydrogen and oxygen in the gas phase; x_{50}, x_{60} are inlet values of x_5 and x_6, respectively; $k_{\pm1}$, $k_{\pm2}$, $k_{\pm5}$, $k_{\pm6}$ the rate constants of the reversible reaction steps in (1); β_1, β_2 the upper limits of the concentrations of hydrogen and oxygen dissolved into the subsurface layer measured in mono-layers; β the conversion factor of concentrations in the gas phase and on the catalytic surface; δ in the residence time. Moreover, the rate constants of the third and fourth steps are as follows:

$$k_3(\boldsymbol{x}) = k_{30}\exp(\mu_{32}x_2 + \mu_{33}x_3 + \mu_{34}x_4),$$
$$k_4(\boldsymbol{x}) = k_{40}\exp(\mu_{42}x_2 + \mu_{43}x_3 + \mu_{44}x_4),$$

where the parameters k_{30}, k_{40} are positive and μ_{ij} ($i = 3, 4$, $j = 2, 3, 4$) are real numbers. Note that the gradients of dissolved reagents are suggested to be small.

After some simplifications we can obtain several reduced models keeping the physical and chemical sense of the catalytic system dynamics and peculiarities being of high importance to the complex irregular behavior. The three-variable version of the kinetic model (2) looks as follows:

$$\dot{x} = \mu f(x, y), \qquad \dot{y} = g(x, y, z), \qquad \dot{z} = \varepsilon h(x, y, z), \tag{3}$$

where $x = x_1$, $y = x_2$, $z = x_4$ (or $z = x_3$). The time constants ε and μ express the idea that not all variables will evolve on the same timescale. In general, $0 < \varepsilon \ll \mu \ll 1$, which expresses the experience that y evolves on the fastest time scale while x and z are identified as intermediate and slow variables, respectively. This model has served as an important motivation for the simplest possible geometrical interpretation of weakly stable dynamics frequently encountered in non-linear heterogeneous catalytic reactions [4].

3. One-parameter family of two-variable dynamical systems

We shall first study a one-parameter two-variable dynamical subsystem of (3) with the parameter z, $0 \leq z \leq 1$:

$$\dot{x} = \mu f(x, y), \qquad \dot{y} = g(x, y, z). \tag{4}$$

As an example, consider the planar system for the catalytic surface coverages by hydrogen and oxygen adsorbed

$$\dot{x} = K_1(1-x-y)^2 - K_{-1}x^2 - 2K_{30}\,\mathrm{e}^{\mu_3 y}x^2y, \tag{5}$$

$$\begin{aligned}
\dot{y} &= K_2(1-x-y)^2 - K_{-2}y^2 - K_{30}\,\mathrm{e}^{\mu_3 y}x^2y \\
&\quad -K_{40}\,\mathrm{e}^{\mu_4 y+\mu_5 z}y,
\end{aligned} \tag{6}$$

where $x = x_1$, $y = x_2$, $K_1 = 2k_1x_5$, $K_2 = 2k_2x_6$, and $K_i = 2k_i$ for $i = -1$ and -2, $K_{30} = k_{30}$, $K_{40} = k_{40}x_5$, $\mu_3 = \mu_{32}$, $\mu_4 = \mu_{42}$, $\mu_5 = \mu_{43}$ or $\mu_5 = \mu_{44}$. It should be noted that with introduction of an additional small parameter $\mu = K_1$, when $K_1 \ll K_2$ and y is not small, the system (5)–(6) can exhibit relaxation oscillations.

4. Phase portraits

In previous papers we studied the system (5)–(6) in details and obtained examples of rather complex dynamics [14]. Phase portraits with up to five steady states and stable and unstable limit cycles are shown in Fig. 1. We found the various phase portraits A–F and M–P of the system (5)–(6) as the parameters K_1, K_2 vary as given in Table 1.

Two cycles, one of which is stable while the other is unstable, exist around the unique stable steady state at $K_1 = 0.005$, $K_{-1} = 0.001$, $K_2 = 0.15$, $K_{-2} = 0.002$, $k_{30} = 500$, $k_{40}\,\mathrm{e}^{\mu_5 z} = 1.5$, $\mu_3 = -80$, $\mu_4 = -10$ (picture G). If we fix all parameters and let K_2 vary, then for $K_2 \in [0, 0.19]$ the only one steady state exists and it is a sink. But at $K_2 = 0.1033$ two full grown limit cycles (stable and unstable) suddenly appear and the system has the phase portrait like G for $K_2 > 0.1033$. Such phenomenon could be called as "a blue sky bifurcation" [15].

The unstable limit cycle shown in the picture H takes place at $K_1 = 0.0004$, $K_{-1} = 0.01$, $K_2 = 0.07565$, $K_{-2} = 0$, $k_{30} = 10$, $k_{40}\,\mathrm{e}^{\mu_5 z} = 2$, $\mu_3 = -30$, $\mu_4 = -13$. For the same K_{-2}, k_{30}, $k_{40}\,\mathrm{e}^{\mu_5 z}$, μ_3, μ_4 and $K_1 = 0.0001$, $K_{-1} =$

Table 1
Parameters K_1 and K_2 for some phase portraits shown in Fig. 1

	A	B	C	D	F	M	N	O	P
K_1	1.3	2.45	1.3	2.3	2.45	1.1	1.1	1.16	2.45
K_2	60.8	112.2	82.238	110.0	113.681	91.9175	91.96	95.3437	114.1

The other parameters are as follows: $K_{-1} = 0.1$, $K_{-2} = 0.49$, $k_{30} = 1000$, $k_{40}\,e^{\mu_5 z} = 2000$, $\mu_3 = -21$, $\mu_4 = -13.5$.

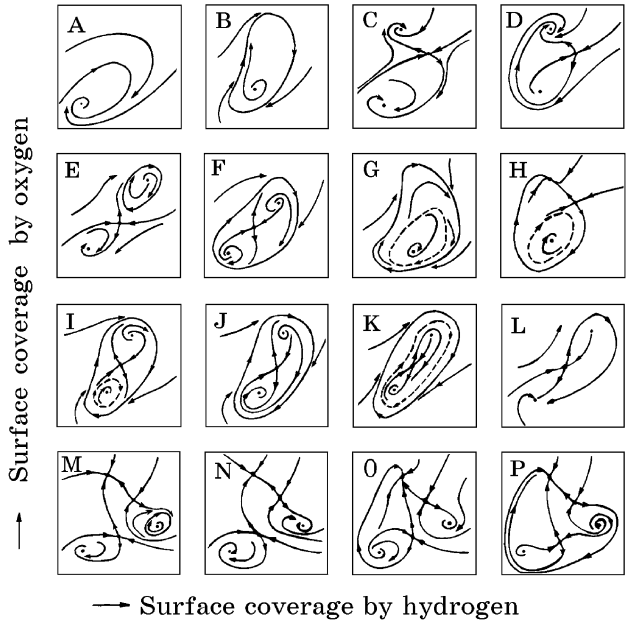

Fig. 1. Phase portraits of the model (5)–(6) in the (x, y) plane. Unstable limit cycles are shown as dashed curves.

10^{-6}, the pictures I, J, K and L arise consecutively while decreasing K_2 from 0.076 to 0.0742. At $K_1 = 0.2$, $K_{-1} = 0.0025$, $K_2 = 15$, $K_{-2} = 0$, $k_{30} = 100$, $k_{40} = 2$, $\mu_3 = -30$, $\mu_4 = -13$, $\mu_5 = 10$, the phase portraits change as A → C → E → B → A upon parameter z increasing from 0 to 1.

Fig. 2 shows the diagram of possible transitions between different phase portraits of Fig. 1 by means of the simplest steady states bifurcations and the simplest periodic orbits bifurcations (so called bifurcations of the unit co-dimension). Detailed description of bifurcations concerned is given in [14]. We will not discuss the completion of this phase portraits collection in other ways then to note, that here the harmonic oscillations occurring in the Hopf bifurcation can become relaxation oscillations. Hence, the local analysis cannot be expected to provide complete information on the possible system dynamics.

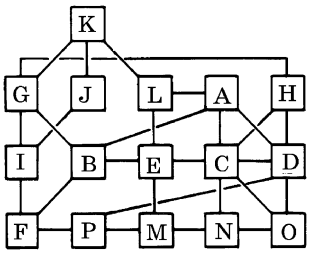

Fig. 2. The scheme of possible transitions among the phase portraits shown in Fig. 1 by local and global bifurcations.

5. Relaxation oscillations

Suppose now that $K_1 \ll K_2$ and $\mu = K_1$ is a small parameter in (5)–(6). If y is not small then we have $|\dot{x}| \ll |\dot{y}|$ except in a neighborhood of the curve $g(x, y, z) = 0$. Therefore, the family of horizontal lines $y =$ constant approximates the flow of (5)–(6) away from $g = 0$ increasingly well as $\mu \to 0$. Near the curve $g = 0$, both solution components are comparable and hence, after entering the boundary layer near this curve, the trajectories turn sharply and follow $g = 0$ until they reach a critical point where they must leave the curve $g = 0$ and follow lines $y =$ constant to another point at $g = 0$. Thus any trajectory that starts outside the singular point reaches a neighborhood of the curve ABCD in finite time and stays in that neighborhood forever (see Fig. 3).

An example of relaxation oscillations in the two-variable model is given in Fig. 4. Considering the system (5)–(6) we have discovered that there exists a value z_c such that for z in a small neighborhood of z_c the limit cycle ABCD deforms into a canard A′BCDB′ given in Fig. 5. As z increases (still in the neighborhood of z_c) the head of the canard A′BB′ gets smaller and in the next stage there is the second unstable limit cycle (“a duck EFD without a head”) inside the stable canard limit cycle as given in Fig. 6.

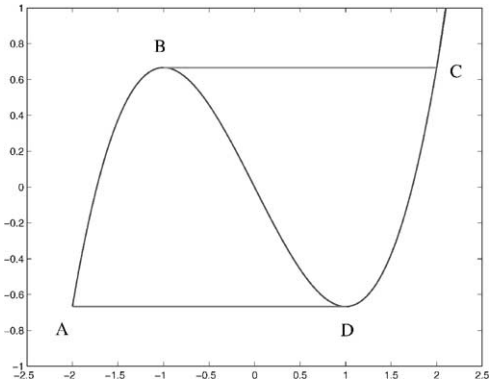

Fig. 3. Limit cycle of the classical relaxation oscillation with the fast motion along BC, DA and slow motion along AB, CD.

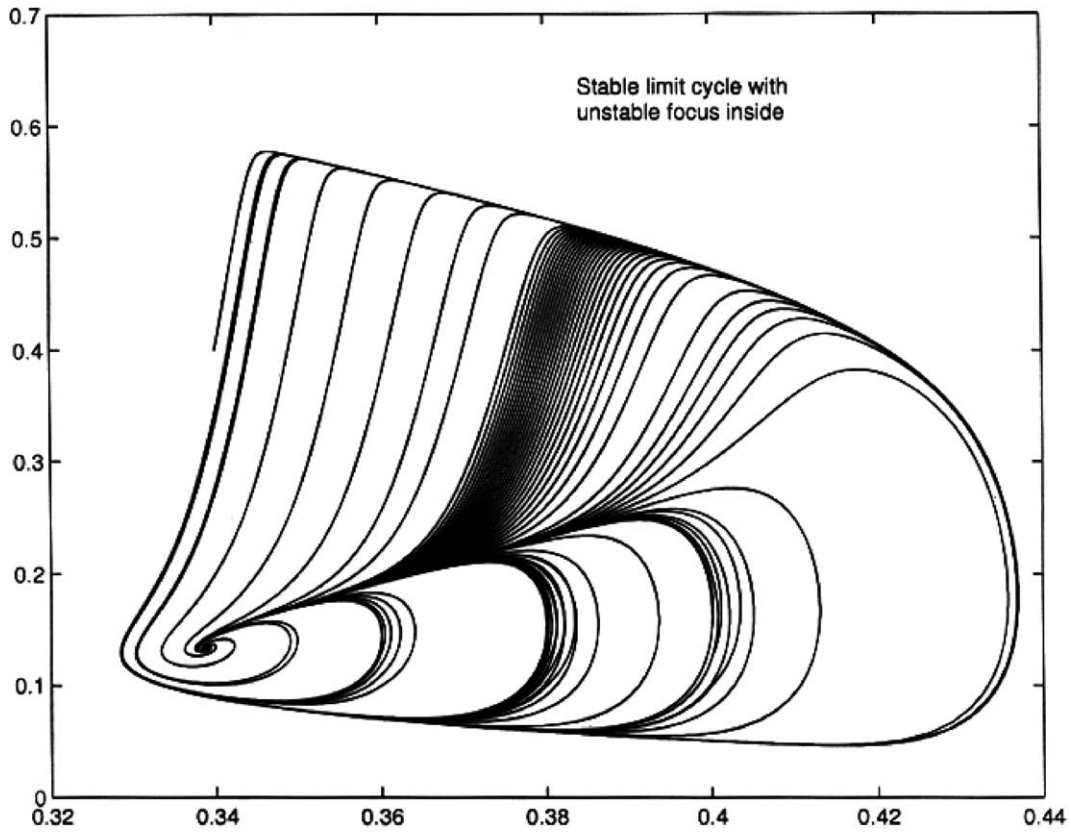

Fig. 4. Example of relaxation oscillations in the system (5)–(6).

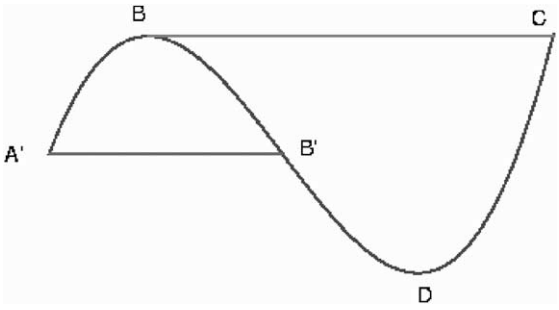

Fig. 5. A canard limit cycle A′BCDB′. Morphology of the canard: A′ is a bill, B′ is a neck, C is a tail.

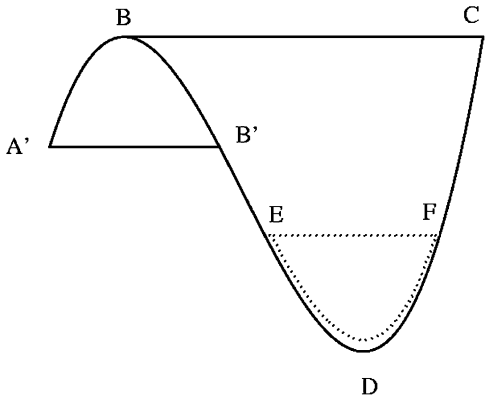

Fig. 6. A canard with the unstable limit cycle inside it.

6. One-parameter family of limit cycles

Now, we describe phase portraits of the model (5)–(6) as the parameter z varies and

$$K_1 = 0.2, \quad K_{-1} = 0.0025, \quad K_2 = 15, \quad K_{-2} = 0,$$
$$k_{30} = 100, \quad k_{40} = 2, \quad \mu_3 = -30, \quad \mu_4 = -13,$$
$$\mu_5 = 10.$$

We would like to point out that the canard configuration indeed occurs in the system (5)–(6). At fist, it is convenient to draw a transition from the Hopf bifurcation to the relaxation oscillations in the one-parameter family of stable limit cycles. The corresponding phase portraits are shown in Fig. 7 where the curves 1 and 2 present harmonic oscillations born in the Hoph bifurcation being closed to $z = 0.3554$, while the cycles 4–9 present relaxation oscillations. It should be pointed out, that in the orbit 10 an important feature is apparent: this limit cycle has already got a canard configuration. The question is: how does the limit cycle disappear when we increase z further? In what follows we shall concentrate on the case that z is in the neighborhood of 0.445 and we shall see that the range of z is extremely small where the canard configuration is observed. More precisely, as $\mu \to 0$ a canard is characterized by

$$z = z_{\mathrm{m}} - \sigma\, \mathrm{e}^{-1/k\mu},$$

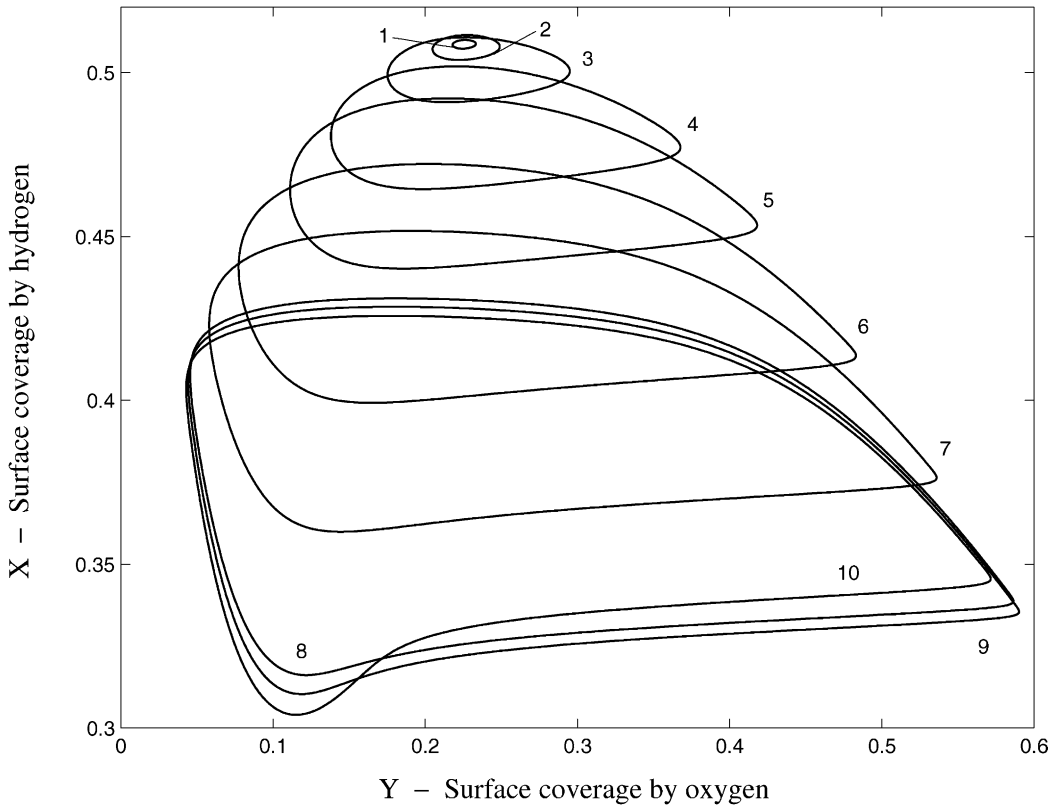

Fig. 7. One-parameter family of the stable limit cycles for different parameter values z in the model (5)–(6): $z = 0.3554$ (1), 0.3560 (2), 0.36 (3), 0.37 (4), 0.38 (5), 0.40 (6), 0.42 (7), 0.44 (8), 0.4425 (9), 0.4452 (10).

where $\sigma > 0$, $k > 0$. The group of French mathematicians called the process of study as "a chase on canards" [8].

7. Stable and unstable supercritical ducks

We established numerically that canard configurations occur when $0.445017 < z < z_m$ with $z_m = 0.445233121773$. The most interesting thing about the canards is the following: in the canard situation a trajectory that comes down along the stable manifold continues for a while along the unstable manifold.

It might be thought that the next Hopf bifurcation occurring as z passes with increasing through a certain value z_H would give degeneration of stable periodic orbits, but in subsequent analysis it was shown that unstable periodic orbits shrink down upon the sink as z decreases towards z_H and no closed orbits exist near this fixed point for $z > z_m$. The corresponding diagram is sketched in Fig. 8. Thus it turns out that there are two breeds of canards in the model (5)–(6).

Now, we focus our attention on the graph of $A(z)$ in the interval $[z_c, z_m]$, where $A(z)$ measures the area enclosed by limit cycles. The phase portraits for these parameter values

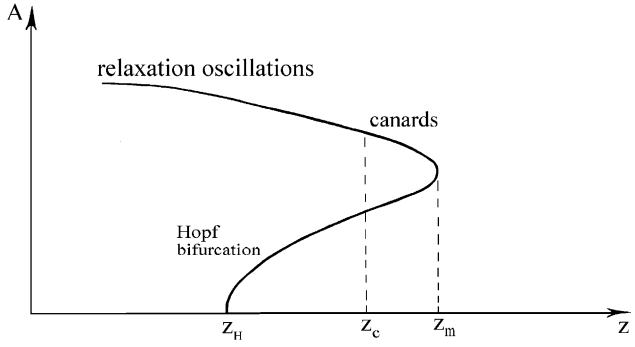

Fig. 8. Canards disappearance with a stable singular point at $z = z_m$. "A" measures the area enclosed by the limit cycles.

are shown in Fig. 9. In particular, note that for each z-value there is an unstable limit cycle inside the stable limit cycle. A singular point of the system (5)–(6) is now stable and there are ducks as stable limit cycles (curves 2–5, Fig. 9) with the growing supercritical ducks without heads as unstable limit cycles (curves 2′–5′, Fig. 9) It is the most complicated part of ducks phenomenology. As we increase z further the two cycles coalesce at z_m between curves 5 and 5′ ("a blue sky bifurcation" occurs). It is not difficult to see that for $z > z_m$ trajectories spiralize toward the singular point.

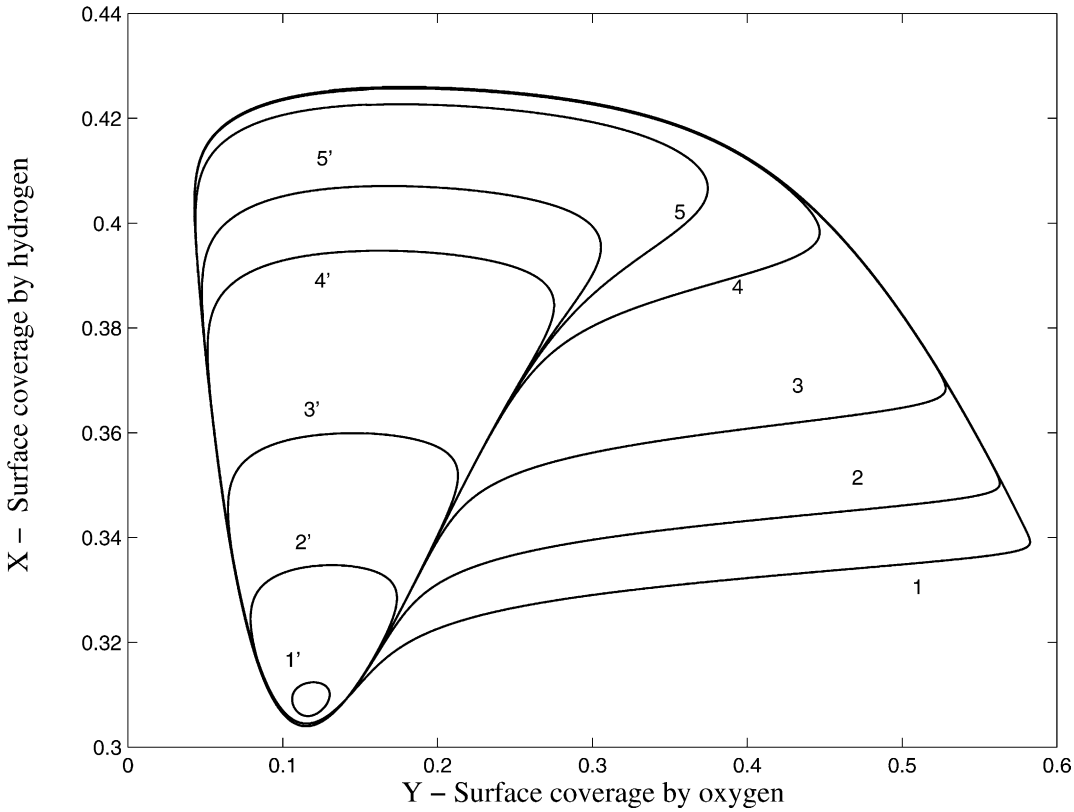

Fig. 9. Ducks for $z = 0.445017$ (1,1′), 0.445224 (2,2′), 0.445233 (3,3′), 0.44523312 (4,4′), 0.445233121770 (5,5′) in the model (5)–(6).

8. Sensitive dependence on initial conditions

In classical strategies for non-linear oscillations analysis the stress is on the individual solution curves and their properties. Here we shall be more concerned with families of such curves (bundles of trajectories) and hence, with the global behavior of the flow in the phase space of the system considered. Therefore, a global error in long-term numerical integration of ODEs will be of interest. We shall refer to the local expansion of orbits starting arbitrary close together as sensitive dependence on the initial conditions. Studying the problem of the Canards it has became clear that the parametric sensitivity appears in such phenomenon in Non-Standard Analysis as a tunnel.

A whirlpool is a trajectory bundle, when trajectories were perceptibly far from each other but then become infinitely close. *A shower* is a trajectory bundle, when trajectories were infinitely close to each other and then diverged perceptibly far. *A tunnel* is a trajectory bundle, which behaves first like a whirlpool (tunnel entry) and then like a shower (tunnel exit). As an example we demonstrate the situation “a shower” in the middle of Fig. 4.

In Fig. 9, we illustrate the sensitive dependence on initial conditions. For concreteness, cycles 2′–5′ and 2–5 form a tunnel with growing length as z increases. The attraction basins of the corresponding stable limit cycles are so narrow that small perturbations (numerical or physical) prevent typical orbits from achieving periodic asymptotic behavior.

Thus, considering the model (5)–(6) of catalytic hydrogen oxidation, we have discovered that there exists a surface state of the catalyst for which the system shows extremely high sensitivity to the initial conditions (the surface coverages by hydrogen and oxygen or concentration of a compound dissolved into subsurface layer) from a small neighborhood of this state. This situation is rather unusual but we think that this phenomenon is one of the keys to weakly stable dynamics in three-variable systems.

9. Weakly stable dynamics

The system (3) can be embedded in a one-parameter family of dynamical systems

$$\dot{x} = \mu f(x, y, \kappa), \qquad \dot{y} = g(x, y, z, \kappa), \qquad \dot{z} = \varepsilon h(x, y, z) \tag{7}$$

with the bifurcation parameter $\kappa = x_5$ being partial pressure of hydrogen in the gas phase. Now we shall vary κ to obtain a system with weakly stable dynamics [11]. Numerical integration of the system (7) appears to yield trajectories that are not asymptotically periodic (see Fig. 10). In fact in some cases we observe chaotic orbits followed by asymptotically

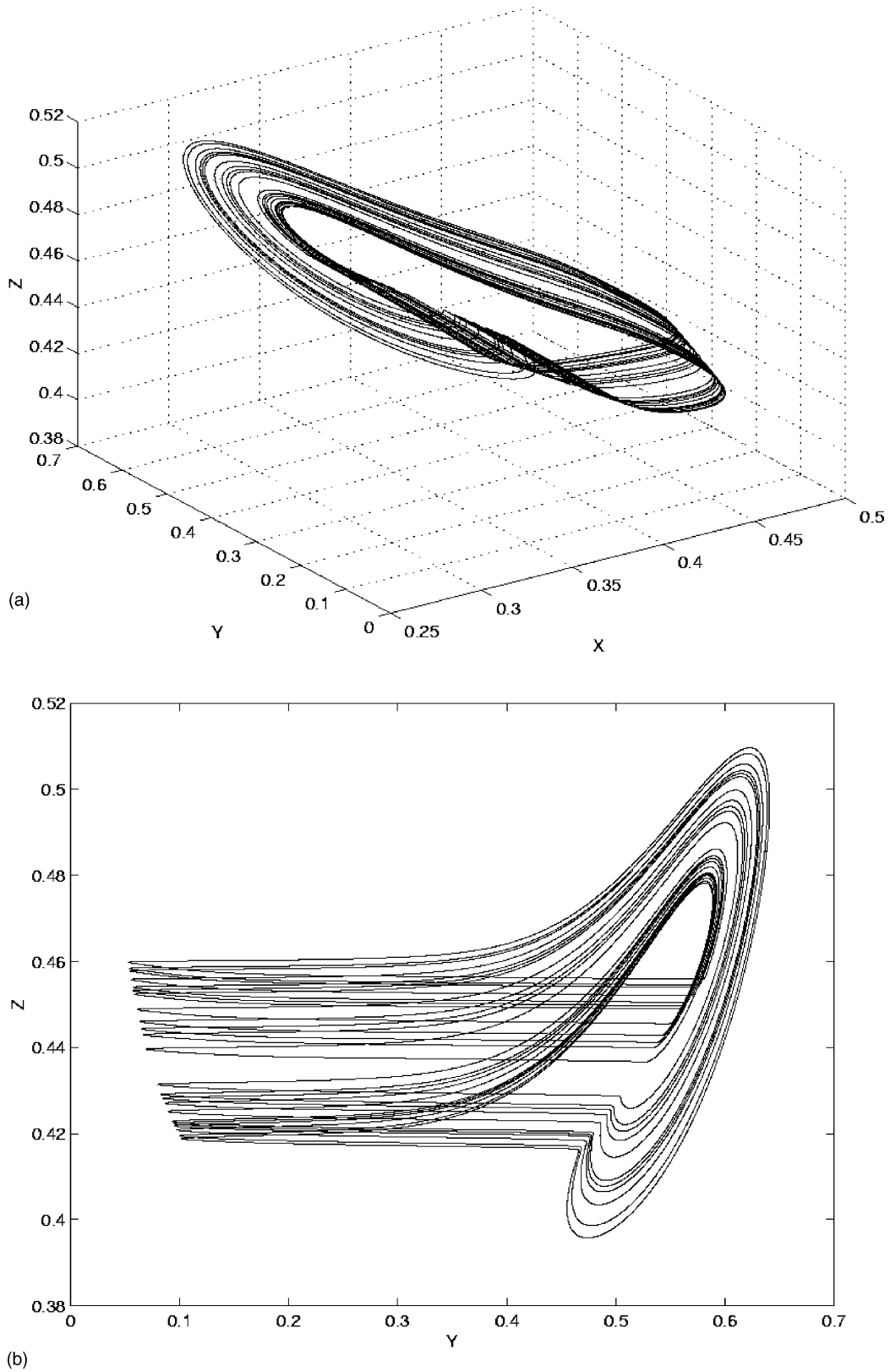

Fig. 10. Weakly stable dynamics in the system (7): phase-portrait (a) and its projection on the plane "surface coverage by oxygen adsorbed, *Y*—concentration of oxygen dissolved into catalyst sublayer, Z" (b). $K_1 = 0.152$, $K_{-1} = 0.008$, $K_2 = 20$, $K_{-2} = 0$, $k_{30} = 100$, $k_{40} = 2$, $\mu_3 = -30$, $\mu_4 = -12$, $\mu_5 = 10$, $\varepsilon = 0.0024$, $k_{-6}/k_6 = 7.88$.

periodic motions. Since we enter a realm in which the theory remains in an unsatisfactory state, we would like to point out some reasons of weakly stable behavior appearance in the system (7):

(i) an attractor containing Mobius band is presented in the phase space of the system (7);
(ii) a subregion on the attractor exists with a high sensitive dependence on the initial conditions; note that in the model (7) it occurs in a neighborhood of the canard configuration for the one-parameter family (5)–(6);
(iii) infinite times the trajectory comes back into this subregion.

It should be noted that both breeds of canards are practically unstable for the numerical integration since a quantity $\ln[\mathrm{tr}(A^{\mathrm{T}}(t)A(t))]/(2t) \gg 1$ on the unstable manifolds of canards, where $A(t)$ is the Jacobian matrix of the system (7). Therefore, a global error in numerical integration of canards trajectories strongly grows, that inhibits the precise prediction of the future of the dynamical system in attractor with the properties (i)–(iii).

10. Global error in long-term numerical integration

Here it might be partinent to determine *a global error in long-term numerical integration* of ordinary differential equation

$$\dot{\xi} = F(\xi), \qquad \xi(0) = \xi_0, \qquad 0 \le t \le T. \tag{8}$$

Having defined t_n for $n = 0, 1, 2, \ldots$ and solved some finite-difference or other discrete equation that approximates (8), we would obtain an approximation ζ_n of the true solution $\xi(t)$ at each t_n. Defining $e_n = \zeta_n - \xi(t_n)$, we shall call e_n the global discretization error at the end-point of the interval $[0, t_n]$. Now our aim is to produce some sort of estimate for e_n.

To analyze the global discretization error we consider the local errors of approximation as result of a perturbation of the original initial problem (8). We regard the approximate solution $\zeta(t)$, where $\zeta(t_n) = \zeta_n$ as the exact solution of the initial value problem

$$\dot{\zeta} = F(\zeta) + \delta\rho(t, \zeta), \quad \zeta(0) = \zeta_0. \tag{9}$$

Using the function $\delta\rho(t, \zeta)$ we simulate the finite-difference scheme, where $\delta\rho(t, \zeta)$ is the local error of the numerical discretization process, and δ a small parameter that depends of the grid step. As the approximate value of $\zeta - \xi$ we will use the first and the only term of the asymptotical decomposition $\zeta(t) - \xi(t) = \delta\eta(t) + \delta\omega(t, \delta)$, where $\omega(t, \delta) \to 0$ as $\delta \to 0$ and $t \in [0, T]$. The function $\eta(t)$ is the solution of the initial value problem

$$\dot{\eta} = F_\zeta(\zeta(t))\eta + \rho(t, \zeta), \quad \eta(0) = 0, \tag{10}$$

where $F_\zeta(\zeta(t))$ is the Jacobian matrix of first partial derivatives of the function F.

The dynamic behavior of the global error in long-term numerical integration of the system (7) by means of embedded Runge–Kutta methods is shown in detail in our recent paper [12].

Acknowledgements

This research was supported in part by the International Association for the promotion of co-operation with scientists from the New Independent States of the former Soviet Union—INTAS grant no. 99-01882. We are grateful to our students Kiseleva Anna (Novosibirsk State University) and Chumakova Lyubov (University of Wisconsin-Madison, USA) for active participation in the numerical experiments.

References

[1] M.T.M. Koper, Bifurcations of mixed-mode oscillations in a three-variable autonomous Van der Pol-Duffing model with a cross-shaped phase diagram, Physica D 80 (1995) 72–94.
[2] S.M. Baer, T. Erneux, Singular Hopf bifurcation to relaxation oscillations, SIAM J. Appl. Math. 46 (5) (1986) 721–739.
[3] M.M. Slin'ko, N.I. Jaeger, Oscillating Heterogeneous Catalytic Systems, Studies Surface Sci. Catal., vol. 86, Elsevier, Amsterdam, 1994.
[4] G.A. Chumakov, M.G. Slinko, Kinetic turbulence (chaos) of reaction rate for hydrogen oxidation on metallic catalysts, Dokl. Acad. Nauk. USSR 266 (5) (1982) 1194–1198 (in Russian).
[5] F. Schuth, B.E. Henry, L.D. Schmidt, Adv. Catal. 33 (1993) 51.
[6] R. Imbihl, G. Ertl, Chem. Rev. 95 (1995) 697.
[7] G.A. Chumakov, N.A. Chumakova, French Ducks in Kinetic Model of a Heterogeneous Catalytic Reaction, in: Proceedings of the Fourth Siberian Congress on Industrial and Applied Mathematics INPRIM-2000, Book of Abstracts, Part IV. IM SB RAS, Novosibirsk, 2000, p. 26 (in Russian).
[8] E. Benoit, J.L. Callot, F. Diener, M. Diener, Chasse au Canard, IRMA, Strasbourg, 1980.
[9] W. Eckhaus, Relaxation Oscillations including a Standard Chase on French Ducks, in: A. Dold, B. Eckmann (Eds.), Lecture Notes in Mathematics, Vol. 985, Asymptotic Analysis II—Surveys and New Trends, Springer-Verlag, Berlin, Heidelberg, 1983, pp. 449–491.
[10] V.I. Arnold, Ordinary Differential Equations, MIT Press, Cambridge, MA, 1973 (Russian original, Moscow, 1971).
[11] P. Berge. Y. Pomeu, Ch. Vidal, L'ordre dans le chaos, Hermann, Paris, 1988.
[12] G.A. Chumakov, N.A. Chumakova, On a global error estimate in long-term numerical integration of ordinary differential equations, Selçuk J. Appl. Math. 2 (1) (2001) 27–46.
[13] G.A. Chumakov, M.M. Slinko, V.D. Belyaev, M.G. Slinko, Kinetic model of an autooscillating heterogeneous reaction, Dokl. Acad. Nauk. USSR 234 (2) (1977) 399–402 (in Russian).
[14] G.A. Chumakov, Analysis of Mathematical Models of the Reaction Rate Oscillations in Heterogeneous Catalytic Reactions, Ph.D. thesis, Novosibirsk State University, Novosibirsk, 1985 (in Russian).
[15] J. Guchenheimer, Ph. Holmes, Non-linear Oscillations, Dynamical Systems, and Bifurcations of Vector Fields. Applied Mathematical Science, Vol. 42, Springer, New York, 1997.